



Cite this: DOI: 10.1039/d4py00971a

Fast, catalyst-free room temperature production of isocyanate-free polyurethane foams using aromatic thiols†

Maxime Bourguignon,^a Bruno Grignard^{a,b} and Christophe Detrembleur^{id} *^{a,c}

Non-isocyanate polyurethane (NIPU) foams of the polyhydroxyurethane (PHU) type are promising greener alternatives to their conventional isocyanate-based polyurethane counterparts that dominate the foam market. Recently, concomitant organocatalyzed aminolysis and *S*-alkylation of the cyclic carbonates of PHU formulations offered a facile route to produce CO₂ self-blown PHU foams. However, this process was limited to the production of foams of rather low T_g (commonly up to room temperature) and suffered from slow foaming (*i.e.* 30 min) at 120 °C, thus still far from the foaming timeframes (1–10 min) and room temperature (*r.t.*) needed for adaptation to industrial foaming equipment. In this work, we elaborate strategies to accelerate thiol-assisted NIPU foaming in order for it to be complete in 5–10 minutes from *r.t.* reactive formulations under catalyst-free conditions. This is achieved by substituting aliphatic thiols by more acidic aromatic ones, and by adding epoxides as heat release promoters that will accelerate both the foaming and the curing rates. Moreover, flexible, semi-rigid and rigid foams are easily accessible by the choice of the amine comonomer and epoxide additive. This work draws general and simple concepts for greatly speeding-up the self-blowing NIPU process, a crucial step toward decreasing the energetic and production costs, offering potential for retrofitting existing foam production plants.

Received 4th September 2024,
Accepted 25th November 2024

DOI: 10.1039/d4py00971a

rsc.li/polymers

1. Introduction

Polyurethane (PU) foams are essential materials of our modern life with multiple usages as insulation materials, items for comfort and furniture, seats, mattresses, *etc.*^{1,2} With an estimated market growth of 7.4% for the 2022–2027 period,³ the success of PU foams is due to their ease of fabrication from low cost isocyanates and polyols. Besides the formation of urethane linkages by polyaddition of the isocyanate with the polyol, the addition of some water within the reactive formulation causes hydrolysis of the isocyanate. This reaction furnishes an amine that participates in PU network construction *via* urea linkage formation, with CO₂ acting as the blowing agent.⁴ These features make the foam production compatible with continuous slabstock foaming (*e.g.* for producing mattresses) or reactive injection molding (RIM; *e.g.* for preparing foams of complex shapes such as car seats and decorative objects). Nevertheless, due to their acute toxicity,^{5,6} isocyanates

face restrictions to their use by REACH.⁷ In addition, PU production also faces recent EU policies on decarbonization of the plastics sector that encourage the utilization of raw chemicals derived from bio-renewables and/or gaseous waste effluents such as CO₂.⁸ Therefore, isocyanate-free pathways for the production of these irreplaceable products that will answer the sustainability goals of Europe are intensively sought. In the last decade, polyamine/poly(cyclic carbonate) copolymerization, leading to poly(hydroxyurethane)s (PHUs),^{9–12} has imposed itself as one of the main alternatives to conventional PU thermosets, particularly for producing foams, coatings and adhesives.^{13–19} The foaming of PHUs has been explored using a physical blowing agent such as Solkane²⁰ – a fluorinated solvent that contributes to global warming – or supercritical CO₂.²¹ Other recent concepts also use inorganic carbonate salts (K₂CO₃, NaHCO₃) in synergy with acids (maleic or acetic acid) as the source of CO₂ to formulate foamed materials from reactive formulations.^{22,23} The first self-blown PHU foams were described with Momentive MH15, a poly(methylhydrogensiloxane) reactive against amines, that releases *in situ* highly flammable H₂ as the blowing agent.^{24–27} However, all these foaming approaches still face environmental or safety issues and are far from achieving a PU self-blowing technology for which one of the monomers, *i.e.* the isocyanate, serves both for the polymer chain construction and as a source of the blowing agent.

^aCenter for Education and Research on Macromolecules (CERM), CESAM Research Unit, University of Liege, Sart-Tilman B6a, 4000 Liege, Belgium.
E-mail: christophe.detrembleur@uliege.be

^bFRITCO2T Platform, University of Liege, Sart-Tilman B6a, 4000 Liege, Belgium

^cWEL Research Institute, avenue Pasteur, 6, 1300 Wavre, Belgique

† Electronic supplementary information (ESI) available. See DOI: <https://doi.org/10.1039/d4py00971a>

Recently, our group developed two popular strategies for producing CO₂-self-blown PHU foams. The most recent one involved the partial hydrolysis of 5-membered cyclic carbonates catalyzed by (organo)bases that initiated the foaming in a moderate time frame (about 30 min) at 100 °C.^{28,29} In the subsequent study, this process was improved for a rapid foaming (a few minutes) from room temperature formulations,³⁰ reaching a foaming performance very close to industrial ones. This was achieved by adding some epoxide to the formulation that had a dual role, to create the additional exotherm needed to reach the foaming zone (85–100 °C) and to introduce additional crosslink nodes needed to rapidly fix the foam and avoid its collapse. The second method capitalized on the ambivalent reactivity of the cyclic carbonates. The nucleophilic attack of the carbonyl site by the amine of the formulation delivered hydroxyurethane linkages while a competitive *S*-alkylation reaction occurred *via* attack of the methylene site by (masked) thiols added to the formulation, leading to thioether bond formation and CO₂ release promoting the self-blowing of the matrix.^{31–35} This strategy mimics the polyurethane chemistry as the reaction leading to the formation of the blowing agent also contributes to the foam cross-linking. Moreover, the structure of the thiol also influenced the foam properties as it was incorporated into the polymer network. However, the foaming conditions (several hours at 80–100 °C) were still far from the conventional PU ones (1–15 min) or the PHU ones produced by the optimized water-induced self-blowing procedure described above. Strategies to accelerate the PHU self-foaming promoted by thiols have primarily focused on modifying the process itself as exemplified by Torkelson.³⁵ The decoupling of the gelation and foaming steps reduced the foaming time from hours to about 30 min, however a high foaming temperature (120 °C) was still required. This was achieved by a short pre-foaming step at 80 °C for 3–6 min to increase the formulation viscosity, followed by foaming for 20 min, at 120 °C. Further decreasing the foaming time while significantly decreasing the formulation temperature was not possible by this process. Recently, Verdejo reported the fast fabrication of thiol-induced CO₂ self-blown polymers from r.t. reactive formulations by designing the partial carbonatation of epoxide (85% of cyclic carbonate and 15% of epoxide) to drive the foaming.³⁶ According to the formulation composition presented in their article and FT-IR analysis, the foams contain a low hydroxyurethane content and are predominantly cross-linked by thioether bonds.

In this work, we address the challenge of rapidly producing PHU foams by the thiol-assisted self-foaming process from room temperature (r.t.) formulations. Herein, we explore the influence of the nature of the thiols on their ability to undergo *S*-alkylation by reaction with the cyclic carbonate, and thus the foaming. Model reactions carried out with aliphatic and aromatic thiols enable us to understand why the *S*-alkylation is facile with aromatic thiols under catalyst-free conditions. By utilizing some epoxide additives to the formulations, PHU foams were rapidly produced from r.t. formulations without the need for any catalyst. Ultimately, our evaluation of the

foam properties revealed the system's versatility, as it allows the straightforward production of both flexible and rigid foams using aromatic thiols.

2. Experimental

2.1. Products

Trimethylol propane triglycidyl ether (TMPTE, Aldrich, technical grade), butanediol diglycidyl ether (BDGE, Aldrich >95%), DER 332™ (Aldrich), propylene carbonate (Pc, Aldrich, 98%), epoxidized soybean oil (ESBO, Vandeputte), *m*-xylylene diamine (XDA, Aldrich, 99%), 1,2-bis(2-aminoethoxy)ethane (EDR 148, TCI, >98%), tetrabutylammonium iodide (TBAI, Aldrich, 99%), 1,8-diazabicyclo[5.4.0]undec-7-ene (DBU, Sigma Aldrich, 98%), hydrotalcite synthetic (HTC, Mg₆Al₂(CO₃)₂(OH)₁₆·4H₂O, Aldrich), triethylamine (TEA, Aldrich, 99%), 1,3-bis(aminomethyl)cyclohexane (*cis*- and *trans*-mixture) (1,3 BAC, TCI, 98%), benzylamine (Aldrich, 99%), 2,2'-(ethylenedioxy) diethanethiol (**T1**, EDR-diSH, Aldrich, 95%), 1,3,4-thiadiazobenzene-2,5-dithiol (**T2**, bismuthiol, ABCR, 95%), 4,4' thiobisbenzenthioi (**T3**, Aldrich, 98%), thiophenol (**T4**, Alfa Aesar, >99%), and Portafume SG63 (POR, Sibelco Europe MineralsPlus) were used.

2.2. Method and characterization

The **gel contents** were measured in triplicate by incubating foam samples in 20 mL of THF for 24 h according to the following formula: $GC = 100 \times \frac{m_2}{m_1}$, where m_1 and m_2 are the mass before immersion and the mass after immersion and drying, respectively.

The **foam density** was assessed in triplicate by weighing the foam and dividing its mass by its volume.

The **ATR spectra** were recorded using a Nicolet IS5 spectrometer (Thermo Fisher Scientific) equipped with a transmission or a diamond attenuated transmission reflectance (ATR) device. Spectra were obtained in transmission or ATR mode as a result of 32 spectra in the range of 4000–500 cm⁻¹ with a nominal resolution of 4 cm⁻¹. Spectra were analyzed with ONIUM™ (Thermo Fisher Scientific) software. Analyses were carried out on the inner part of the foam after removing the foam skin.

Nuclear magnetic resonance (NMR) spectroscopy. ¹H-NMR analyses were performed on Bruker Avance 400 MHz spectrometers at 25 °C in the Fourier transform mode.

Differential scanning calorimetry (DSC) was performed on a DSC250 TA Instruments calorimeter. The equilibrated T_g was measured on the first ramp of temperature (–40–80 °C, 10 °C min⁻¹). Then, the DSC sample was allowed to stand at 80 °C for 2 h. A second cycle from –40 to 120 °C at 10 °C min⁻¹ was then carried out to measure the T_g of the dried sample.

Scanning electron microscopy (SEM) was realized with a QUANTA 600 apparatus microscope from FEI. The cell size distribution was calculated by mean diameter measurements of at least 100 cells.

Compression measurement. Compression measurement was performed with an Instron machine in compression under a quasi-static deformation mode with an initial deformation rate of 0.0025 s^{-1} on a square sample of around $1.5 \times 1.5 \times 1.5\text{ cm}$ and of known density in triplicate. A force cell of 10 kN was used for a rigid foam and a force cell of 0.5 kN was used for a more flexible foam. The compression modulus was calculated as the linear regression of the steepest part of the stress–strain curve (2% of strain width) of the elastic region (inspired and adapted from Li and Aspden's work).³⁷ The loading–unloading cycle was obtained in a similar way, using the same deformation speed (0.0025 s^{-1}) during the loading and unloading cycle. The hysteresis loss was calculated according to the following formula:

$$\text{Hysteresis loss} = \frac{\text{area loading} - \text{area unloading}}{\text{area loading}} \times 100,\text{³⁸ where}$$

area loading and area unloading are the air under the stress–strain curve until 50% deformation calculated using the “trapz” integration method of the `scipy.integrate` module of `python3.12`.

Water uptake measurement. Samples of 1 cubic centimeter of foam were first dried and weighed before incubation in a climate chamber at 80% relative humidity and 25 °C for 48 h. Then the samples were weighed again and the water uptake was calculated using the formula:

$$\text{water uptake} = 100 \times \frac{m_2 - m_1}{m_1}, \text{ where } m_1 \text{ and } m_2 \text{ are the mass of the dried sample and the mass after incubation at controlled humidity, respectively.}$$

2.3. Procedure for thiol-induced foaming

Classical foaming procedure. TMPTC (5 g, 5CC = 34.5 mmol) and the thiol (SH = 8.6 mmol) were mixed together, then DBU (260 mg, 1.7 mmol) and XDA (1750 mg, $\text{NH}_2 = 25.7\text{ mmol}$) were added in this order in a square silicon mold ($S = 16\text{ cm}^2$). The mixture was then mechanically mixed for 1 min. The mold was placed in a preheated oven at 100 °C. The foam was cured for 3 h at 100 °C. The thiol was chosen from 2,2'-(ethylenedioxy)diethanethiol (EDR diSH, **T1**, 760 mg), 1,3,4-thiadiazole-2,5-dithiol (bismuthiol, **T2**, 650 mg) or 4,4'-thiobisbenzenthioi (**T3**, 1.08 g). 5CC, NH_2 , and SH respectively state the number of cyclic carbonate, primary amine, and thiol functional groups in the molecule.

Fast foaming procedure. TMPTC (5 g, 5CC = 34.5 mmol) was preheated in a square silicone mold ($S = 16\text{ cm}^2$) at 100 °C until it reached this temperature. Thiol **T1** (760 mg), **T2** (650 mg) or **T3** (1.08 g) (SH = 8.6 mmol) and DBU (260 mg, 1.7 mmol) + XDA (1750 mg, $\text{NH}_2 = 25.7\text{ mmol}$) were preheated separately at 100 °C for 10 min. Thiol was first added to TMPTC and briefly mixed before the diamine/DBU mixture was poured into the mold. The mixture was then mixed mechanically for 0.5 min in the oven or until foaming started. The foaming was allowed to proceed at 100 °C for 5 min, 15 and 30 minutes. The experiment was repeated without adding DBU or using an excess of XDA (2350 mg, $\text{NH}_2 = 34.5\text{ mmol}$). 5CC, NH_2 , and SH respectively state the number of cyclic carbonate, primary amine, and thiol functional groups in the molecule.

Room temperature foaming procedure. In a plastic (PE) bottle of 8 cm height and 6 cm diameter, TMPTC (17.9 g, 5CC = 124 mmol) and epoxide (epoxide function = 124 mmol) were mixed together until a homogeneous mixture was obtained. The diamine ($\text{NH}_2 = 186\text{ mmol}$) was then added and mixed for 30 seconds until homogenized. Finally, the thiol (SH = 62 mmol) was added and briefly mixed for 15 s. The exotherm was measured with a Martindale DT173 temperature probe throughout the reaction time. The probe was introduced at the center of the formulation. When the formulation reached 80–100 °C, the formulation was briefly mixed manually with a spatula to favor good homogeneity of the thiol in the formulation until the foam started to expand. The foam was allowed to cure until it had spontaneously cooled to room temperature. 5CC, NH_2 , and SH respectively state the number of cyclic carbonate, primary amine, and thiol functional groups in the molecule. We recommend carrying out these experiments with caution, as they cause significant exotherms during foaming. The described formulation compositions have been optimized to provide the desired exotherm for the target foam volume. When targeting other volumes of foams, the formulations have to be adapted to control the exotherm, as is usually done in conventional PU foaming.

Model reaction between thiol and propylene carbonate. Propylene carbonate (Pc, 0.51 g, 5 mmol), thiophenol (0.55 g, 5 mmol) and triethylamine (0.5 g, 5 mmol) were preheated at 100 °C for 5 min in an oil bath. All the components were then mixed and allowed to react for 5 min at 100 °C in a sealed tube. Three drops of the mixture were collected and solubilized in 700 μL of deuterated DMF in a NMR tube that was rapidly cooled to $-20\text{ }^\circ\text{C}$ to quench the reaction before $^1\text{H-NMR}$ analysis. The experiment was reproduced using 1-butanethiol (0.45 g, 5 mmol). The results are presented in Fig. 2.

Measurement of the exotherm of the amine-thiol salt formation. Thiol (SH = 13.7 mmol) was placed in a silicon mold of $h = 30\text{ mm}$, $d = 15\text{ mm}$ (wall thickness = 1 cm), then *m*-XDA (0.94 g, 13.7 mmol) was added to the thiol and briefly mixed for 10 seconds. Temperature was measured with a Martindale DT173 temperature probe along the reaction time. The results are presented in Fig. 8.

Measure of the exotherm of the thiol-epoxide reaction. Thiol (SH = 13.7 mmol) was placed in a silicon mold of $h = 30\text{ mm}$, $d = 15\text{ mm}$ (board width = 1 cm), then 1,2-epoxydodecane (2.52 g, 13.7 mmol) was added to the thiol and briefly mixed for 10 seconds. The temperature was measured with a Martindale DT173 temperature probe throughout the reaction time. The results are presented in Fig. 8.

Measurement of the exotherm of the thiolate salt-epoxide reaction. Thiol (SH = 13.7 mmol) was placed in a silicon mold of $h = 30\text{ mm}$ and $d = 15\text{ mm}$ (wall thickness = 1 cm), then *m*-XDA (2.82 g, 41.1 mmol) was added to the thiol and briefly mixed for 10 seconds. After total cooling of the mixture to room temperature, 1,2-epoxydodecane (2.52 g, 13.7 mmol) was added to the thiol and briefly mixed for 10 seconds. The temperature was measured with a Martindale DT173 temperature probe throughout the reaction time. The results are presented in Fig. 8.

Model reaction of the thiol/epoxide reaction. In a closed glass vial, 1,2-epoxydodecane (1.2 g, epoxide = 6.5 mmol), thiol (SH = 6.5 mmol) and finally the catalyst were added in this order and then mixed briefly at room temperature before being thermostated for 15 min at r.t. Then a sample was picked out, directly solubilized in CDCl_3 and maintained at $-20\text{ }^\circ\text{C}$ to avoid any further reaction. The sample was then analyzed by ^1H NMR. It was noted that instead of using 4,4-thiobisbenzthiol that presents very low solubility and bad dispersion in this epoxide, we used thiophenol as a model aromatic thiol compound. The results are presented in Fig. 8.

3. Results and discussion

3.1. Aromatic thiol-induced self-blown PHU foams at $100\text{ }^\circ\text{C}$

Based on the hard and soft acid base theory of Pearson, the reactivity of *S*-nucleophiles is dictated by an interplay between the acidity and the charge delocalization of the sulfur electrons,³⁹ and aromatic thiols should present higher reactivity vs. cyclic carbonates than aliphatic ones. To assert this, the widely used aliphatic, 2,2'-(ethylenedioxy)diethanethiol (**T1**; Fig. 1A),^{32,34,35,40} taken as a reference, was compared with an aromatic thiol (*i.e.* bismuthiol (**T2**)⁴¹ or 4,4'-thiobisbenzthiol (**T3**)) in a typical formulation composed of a CO_2 -based tricyclic carbonate (TMPTC), a diamine (XDA) and DBU as the catalyst ($[\text{5CC}]/[\text{NH}_2]/[\text{SH}]/[\text{DBU}]$ in a ratio of 1/0.75/0.25/0.05). The three formulations were tested according to two different foaming procedures and validated for the water-based self-foaming process: (1) preheating the components at $100\text{ }^\circ\text{C}$ before mixing them for foaming (fast foaming procedure), and (2) mixing the components at r.t., followed by heating the formulation at $100\text{ }^\circ\text{C}$ (classic foaming process).²⁸

When using the classic foaming procedure, aliphatic thiol **T1** showed a delayed foam expansion in comparison with the aromatic thiols with a time to initiate the expansion of 30 min for **T1**, 20 min for **T2** and 10 min for **T3** (Fig. 1B1). The foam density was also higher when using **T1** (355 kg m^{-3} for **T1** vs. 203 and 310 kg m^{-3} for **T2** and **T3**, respectively) with similar gel contents ($\text{GC}_{\text{T1}} = 92\%$, $\text{GC}_{\text{T2}} = 90\%$, $\text{GC}_{\text{T3}} = 86\%$) (Fig. 1C1). The lower foam densities as well as the shorter foaming times obtained with the aromatic thiols were assumed to be the result of the faster *S*-alkylation of the cyclic carbonate, promoting faster production of the blowing agent together with faster cross-linking. Importantly, despite both aromatic thiols being solid compounds, **T2** and **T3** were easily dispersed in the PHU formulation and became soluble at the foaming temperature. Moreover, **T2** is available on a large scale and at low cost. They are also more convenient to use as they are almost odorless.

Remarkably, when applying the fast foaming procedure, the foaming started after only 15 seconds with **T2** and instantaneously with **T3**, and complete foam expansion was obtained after 2 min with **T2** and 1 min with **T3** (Fig. 1B2). PHU foams with a high gel content ($>90\%$) and densities of 185 (with **T2**) and 166 kg m^{-3} (with **T3**) were obtained after 30 min of curing (Fig. 1C2). This is in sharp contrast to the same experiment

carried out with the aliphatic thiol **T1** where the foaming started after 2 min, with an expansion that lasted 10 min, and a final density of 372 kg m^{-3} ($\text{GC} = 86\%$). Importantly, while the formulation containing the aliphatic thiol **T1** did not provide any foam in the absence of the DBU catalyst, we discovered that PHU foams could be produced with **T2** or **T3** under catalyst-free conditions (Fig. 1B3 and C3). The expansion window (the time between the start and end of expansion) was only slightly extended by about 1 min, while similar foam densities and gel contents were obtained. We hypothesized that the diamine monomer (XDA) was sufficiently basic to activate the more acidic aromatic thiols **T2** and **T3**, consequently accelerating the *S*-alkylation rate, and thus the CO_2 formation and foam crosslinking.

To support this hypothesis, we monitored some model reactions by ^1H -NMR spectroscopy (Fig. 2). The first one involved reacting a model cyclic carbonate (propylene carbonate, Pc) with a model aromatic thiol (**T4**, thiophenol) or an aliphatic one (**T5**, 1-butanethiol) in a stoichiometric ratio and under solvent- and catalyst-free conditions (after preheating the two components to mimic the fast foaming process). No reaction occurred after 5 min at $100\text{ }^\circ\text{C}$ in the two cases. When triethylamine (1 eq. vs. propylene carbonate) was added to mimic the basicity of the diamine in the PHU formulation, *S*-alkylation was observed with thiophenol, with a propylene carbonate conversion of 53% after 5 min. No reaction was noted with 1-butanethiol in the presence of NEt_3 . This set of experiments supported the aromatic thiol being activated for the *S*-alkylation by the weak base. The basicity of the diamine comonomer in the PHU formulation was thus sufficient to catalyze the formation of the blowing agent in the presence of the aromatic thiols (**T2** or **T3**).

Despite the gas generation being sufficiently fast to promote rapid expansion of the foam, we observed that 30 min of reaction was needed to reach high gel contents. Indeed, on using a standard formulation (TMPTC, XDA and **T2**; $[\text{5CC}]:[\text{NH}_2]:[\text{SH}] = 1:0.75:0.25$) with the fast foaming process under catalyst-free conditions, the gel content values increased gradually with the reaction time, from 24% after 5 min to 91% after 30 min, with no significant difference in the foam density (142 kg m^{-3}) (Fig. 3A). FT-IR analysis showed that the 5CC conversion was quite low after 5 min with an intense band of the carbonyl elongation at $= 1800\text{ cm}^{-1}$ (Fig. 3B). Although the foam was fully expanded and did not collapse after 5 min, only partial conversion of the cyclic carbonate was noted, leading to a poorly cross-linked structure as evidenced by the low gel content.

To increase the gel content after 5 min of reaction, we slightly increased the amine content from 0.75 to 1 eq. Under these conditions ($[\text{5CC}]:[\text{NH}_2]:[\text{SH}] = 1:1:0.25$), a gel content above 90% was reached after 5 min (Fig. 3A), together with the almost total consumption of 5CC groups as demonstrated by FT-IR (Fig. 3B and Fig. S2[†]). Importantly, the foam (155 kg m^{-3}) was easily and directly demoldable after this short reaction time without the need to cool the whole system (foam and mold). This is particularly relevant for industrial

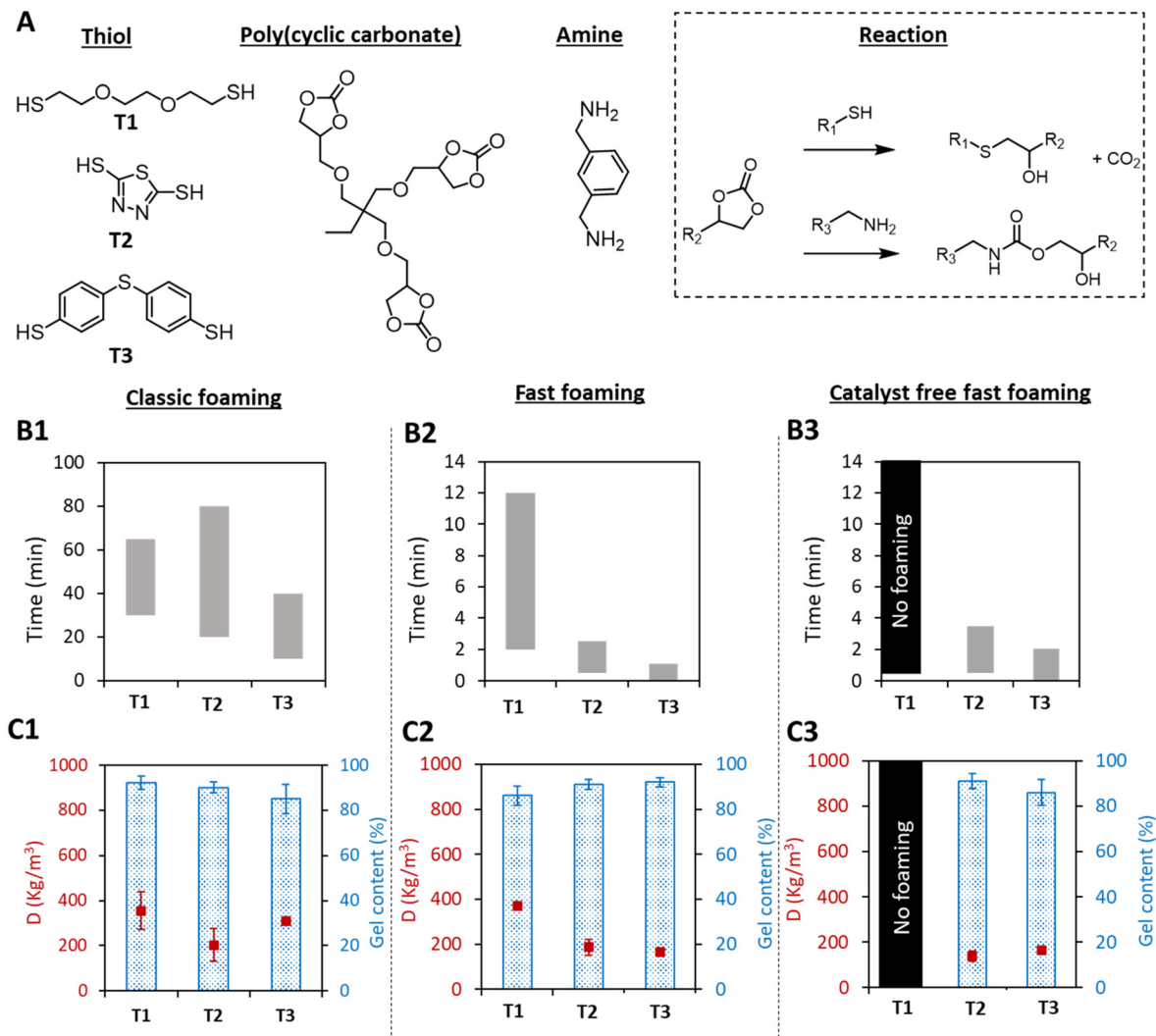


Fig. 1 Thiol-induced self-blown PHU foaming. (A) Structure of the monomers and scheme of both reactions leading to PHU foams. (B) Expansion windows of the foams for the classic procedure (B1, mixing all components at room temperature before heating for 3 h at 100 °C), the fast procedure (B2, preheating the components to 100 °C before mixing them together and then curing for 30 min at 100 °C) and the fast foaming procedure under catalyst-free conditions (B3); T1, T2, and T3 refer to the thiols presented in A. (C). Densities and gel contents of foams obtained by the different foaming procedures (measured after 3 h for C1 and 30 min for C2 and C3). Conditions: TMPTC (5CC = 1 eq.), XDA (NH₂ = 0.75 eq.), thiol (SH = 0.25 eq.), DBU (0.05 eq. for classic foaming and fast foaming 0 eq. for catalyst free fast foaming). Characteristics of the different foams are presented in Table S1.† 5CC, NH₂ and SH state the number of cyclic carbonate, primary amine and thiol groups within the molecules.

applications where a high turnover is required during production, *e.g.* in the RIM process.

Based on this improved formulation ($[5CC]/[NH_2]/[SH] = 1/1/0.25$), we produced a range of PHU foams under catalyst-free conditions in 5 min at 100 °C with two aromatic thiols (T2 and T3) or different diamines (XDA for F1 and F3 or EDR 148 for F2) (Fig. 4 and Table S2†). With T2, exchanging XDA (F2) and EDR 148 did not significantly influence the cell size (1.3 mm; Fig. 4A), the gel content (GC = 93%, Fig. 4C) or the density (155 vs. 156 kg m⁻³). As expected, the most significant difference was observed for the thermo-mechanical properties with a lower T_g (7.9 vs. 34 °C; Fig. 4D) and compression modulus (0.011 vs. 8.3 MPa; Table S3†) for the EDR-based foam compared to the XDA-based one. A flexible foam was thus obtained

with EDR 148 and a rigid one with XDA. Note that for the XDA-based foam, we noticed the abrupt rupture of some rigid cells leading to stress release and giving a saw-tooth shape to the compression curve (Fig. 4B). This unusual shape of the stress/strain curve of F3 was certainly linked to the brittleness of the foam (see Fig. S10† for pictures of the foam before and after compression).

Substituting T2 for T3 (formulation F3, Fig. 4A) delivered inhomogeneous foams with very large cells ($d > 5$ mm), coexisting with smaller ones ($d < 1$ mm). This is due to the higher reactivity of T3 (foam expansion is faster than that with T2 as illustrated in Fig. 5B1–B3) which promoted rapid production of the blowing agent when the matrix was still poorly cross-linked and exhibited an inappropriate viscosity. This could not

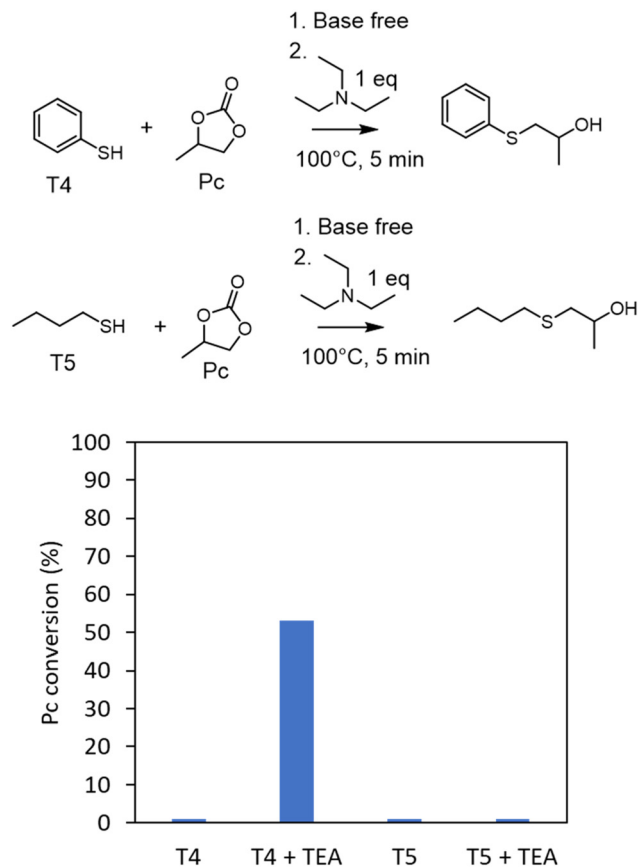


Fig. 2 Propylene carbonate (Pc) conversion when reacted with thio-phenol (T4) or 1-butanethiol (T5) in the presence or absence of triethylamine (TEA) determined by 1-H NMR spectroscopy (see Fig. S1† for NMR spectra). Conditions: propylene carbonate (5 mmol), thiol (5 mmol), TEA (5 mmol), preheating of the components at 100 °C before mixing them, followed by reaction at 100 °C for 5 min in a closed vial.

avoid some coalescence of the growing cells within the matrix. As expected, this foam also showed a rigid character attested by a compression modulus of 2.97 MPa for 124 kg m⁻³ (due to foam heterogeneity, the density of the tested sample differs from the overall density) (F3, Fig. 4B). It is worth mentioning that as well as accelerating the foaming process and getting rid of any catalyst, the use of an aromatic thiol greatly broadened the variety of accessible foams, from flexible to rigid ones. This is an improvement compared to the previous foams obtained with aliphatic di- or poly-thiol^{32,34,35,40} that presented a flexible character with a low T_g (<10 °C), even when prepared from the rigid diamine XDA (entries 1 and 2, Table S1†). However, under more extreme humidity conditions (*i.e.* incubation for 48 h at 80% relative humidity), the use of aromatic thiols failed to significantly reduce the hydroplasticization of the PHU network as shown by the important drop of T_g by more than 30–40 °C in comparison with that under dry conditions (Tables S1 and S2†).

The fast foaming process was also found to be compatible with the presence of different fillers (12 wt% *vs.* TMPTC). The addition of hydrotalcite or Portaflame® (a flame retardant) to

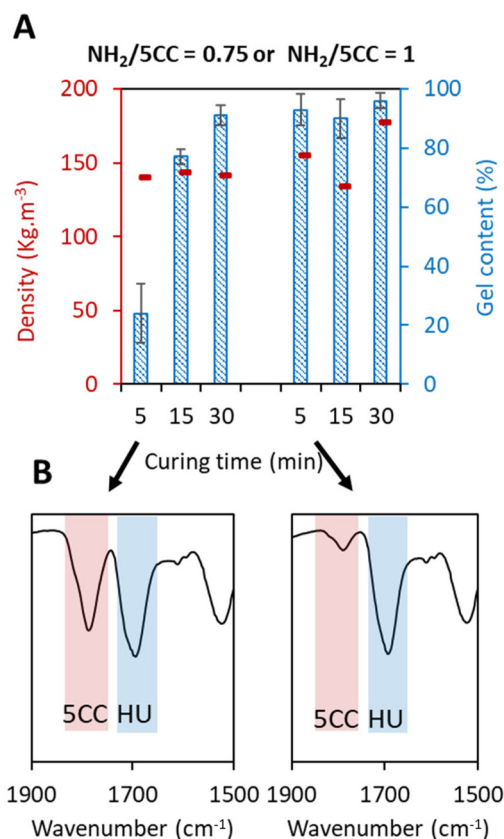


Fig. 3 Comparison of foam properties (GC and density) after 5, 15, and 30 min with two different [NH₂]:[5CC] ratios under catalyst-free fast foaming conditions. (A) Gel content and density values of the foams with different curing times. (B) Infrared spectroscopy after 5 min of curing (complete spectra of interest are depicted in Fig. S2†). Conditions: TMPTC, XDA, T2, catalyst-free, [5CC]/[NH₂]/[SH] = 1/0.75/0.25 or 1/1/0.25, at 100 °C by the fast foaming process.

the T2-based formulation (foam F4 and F5 in Fig. 4) allowed a decrease in the foam cell size and an increase in the homogeneity, as a result of the nucleating effect of the filler, without significantly affecting the GC and density (Table S2†).

3.2. Thiol-induced room temperature foaming

Despite increasing the kinetics of the gas generation, the reactivity of the aromatic thiol/amine was still not sufficient to induce foaming from room temperature reactive formulations. The examples in the previous section showed that the catalyst-free foaming induced by T2 demands temperatures of at least 100 °C and 80 °C when foaming with T3 (entry 7, Table S2†). As the PHU formation is known to be slightly exothermic, we monitored the exotherm of the polymerization when all components of the formulation were mixed at r.t. The goal was to evaluate how far the exotherm was from the foaming zone. Fig. 5 (F8 without epoxide, black curve) shows that the exotherm reached around 60 °C which was not sufficient for foaming.

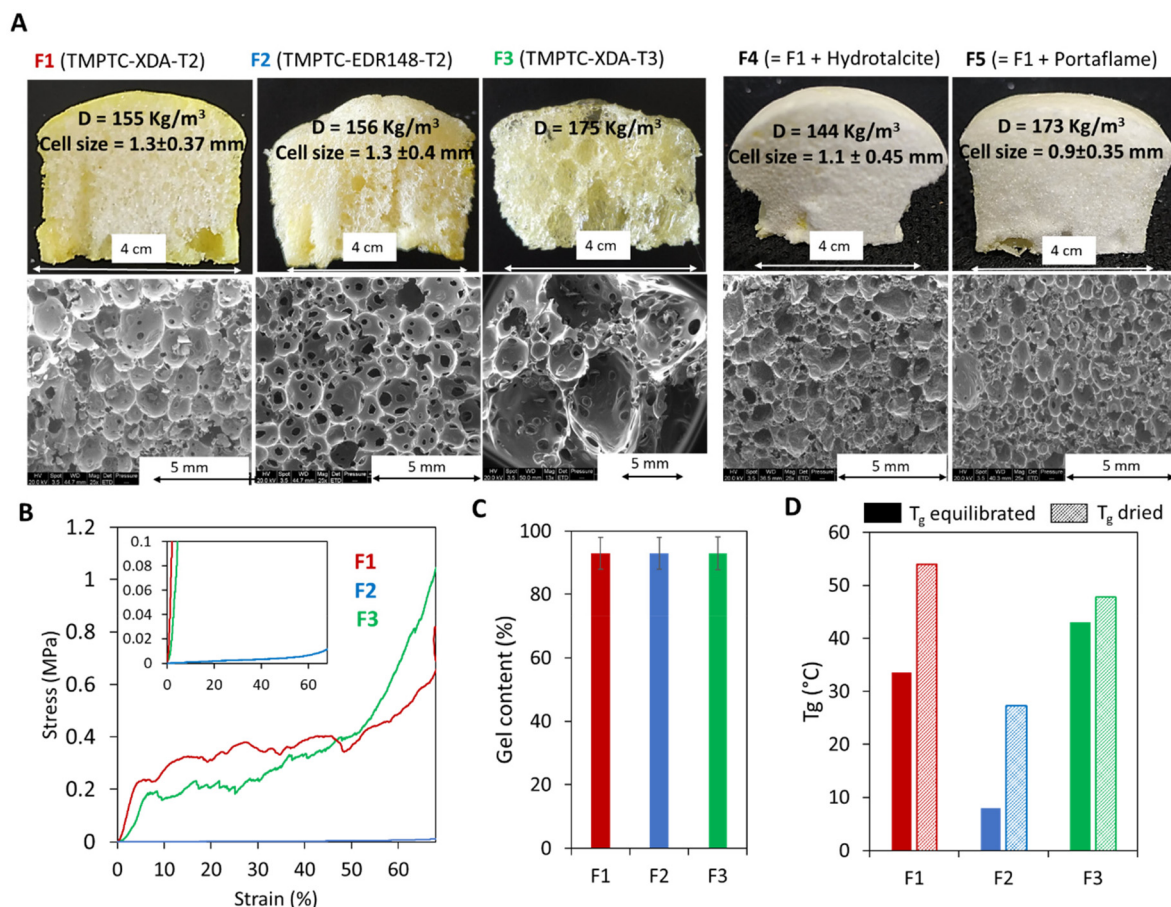


Fig. 4 Characterization of the foams prepared from aromatic thiols. Synthesized with different thiols (T2 for F1, F2, F4, F5, or T3 for F3) or with different amines (XDA for F1, F3, F4, F5 or EDR 148 for F2), without (F1, F2, F3) or with a filler (F4 and F5). (A) Image and morphology of the foams. (B) Compressive curves and (C) gel contents of equilibrated additive-free foams, and (D) glass transition of additive-free foams equilibrated under ambient or dry conditions. Conditions: TMPTC, amine, thiol, catalyst-free, $[5\text{CC}]/[\text{NH}_2]/[\text{SH}] = 1/1/0.25$, 5 min at $100 \text{ }^{\circ}\text{C}$ by the fast foaming process. DSC thermograms are presented in Fig. S3–S9.†

Recently, we presented the cascade exotherm strategy as a solution to improve the foaming of PHU-based formulations induced by hydrolysis.³⁰ In this approach, epoxides were added to the formulation, leading to a rapid increase of the temperature to the foaming zone. The first fast exotherm generated by the aminolysis of the cyclic carbonates rapidly drove the highly exothermic aminolysis of the epoxides, thus leading to fast foaming and crosslinking. Here, we tested this strategy to induce fast foaming from r.t. formulations as the thiol-epoxy click reaction is known to be fast and exothermic.^{42–45} To do so, addition of the diepoxide BDGE (1 eq. of epoxide functional group vs. the 5CC functional group) to the previous formulation containing the aromatic thiol T2 or T3 promoted a rapid increase in the temperature in the corresponding formulations F8 and F7, respectively (up to $170 \text{ }^{\circ}\text{C}$ in less than 5 min, Fig. 5). This exotherm was accompanied by expansion of the matrix in less than 3 min ($d = 229 \text{ kg m}^{-3}$ for F8 and 324 kg m^{-3} for F7, Fig. 6) and cross-linking of the formulation ($\text{GC} = 96\%$ and 93% , Fig. 6). The infrared spectra of the different foams confirmed the PHU nature of the foam with

almost complete disappearance of the carbonyl elongation of 5CC moieties at 1800 cm^{-1} and the appearance of a strongly intense and new signal of hydroxyurethane functions at 1700 cm^{-1} (Fig. S11–S16†). Similar to the observation linked to Fig. 4A, a foam with a rather larger cell size was obtained with T3 (F7) in comparison with T2 (F8) (Fig. 7). Nevertheless, in each case, we noticed a decrease in the cell size in comparison with the foam obtained without epoxide. This is rationalized by faster and denser cross-linking in the presence of the epoxide that stabilized the cell walls during expansion, limiting their coalescence.

Importantly, during the foaming of r.t. formulations, we observed the formation of some aggregates when the aromatic thiols were involved, but not with the aliphatic one. The solid compounds were rapidly formed when all formulation components were mixed at r.t., and they then solubilized when the temperature reached $80\text{--}100 \text{ }^{\circ}\text{C}$. This was rapidly followed by foaming. It was hypothesized that these solid compounds originated from the acid–base reaction between the thiol and the amine, leading to the thiol-amine salt as already observed else-

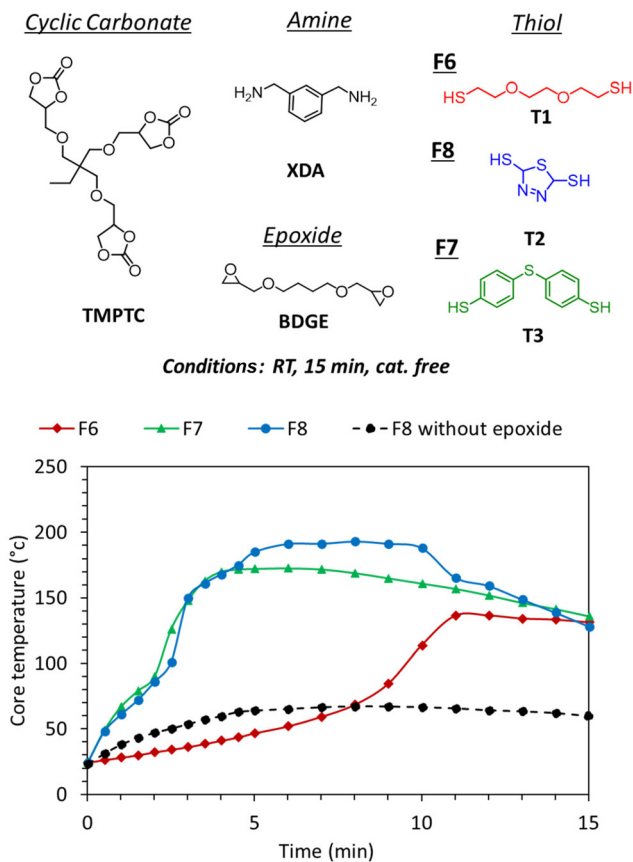


Fig. 5 Room temperature foaming using an epoxide additive for cascade exotherms. Conditions: TMPTC, BDGE, XDA, thiol, [SCC] : [epoxide] : [NH₂ total] : [SH] = 1 : 1 : 1.5 : 0.5.

where.⁴⁶ This was further supported by mixing benzylamine with T2, T3 or thiophenol (T4) without any epoxide, with the formation of a solid compound that precipitated, together with a rapid increase in the temperature despite the low quantity of the reagent (2–3 g scale owing to safety concerns) (Fig. 8B). This was in sharp contrast to the results obtained with the aliphatic thiol T1 that did not show any precipitate nor any exotherm when mixed with the amine (Fig. 8B). This directly explains the important delay observed between the exotherm with F7 or F8 (with aromatic thiol) and F6 (with aliphatic thiol), the latter requiring three times more time to reach 100 °C (~9 min vs. ~3 min) during the foaming procedure (Fig. 5). This difference between the various thiols was explained by the higher acidity of the aromatic thiols vs. the aliphatic one.

Thiols are also known to react with epoxides, and this thiol epoxy-click reaction might be involved in the curing process. This reaction is however generally efficient at a temperature higher than 60 °C.^{42,43} We decided to test for the occurrence of this reaction using model 1,2-epoxydodecane with the aliphatic thiol T1, the aromatic thiol T3 or the model thiophenol (T4) at r.t. In all cases, no exotherm was observed (Fig. 8B, blue curves) and the ¹H-NMR analysis of the reaction medium after

15 min at r.t. showed no epoxide consumption (Fig. 8C; T3 was not tested due to its poor dispersibility in the epoxide). On the other hand, the reaction proceeded well when catalyzed by DBU (0.05 mol%) and was faster with aromatic thiols (96% conversion for T4 instead of only 28% for T1; Fig. 8C). Surprisingly, the reaction of bismuthiol (T2) with the epoxide occurred rapidly from r.t. with an important exotherm (more than 100 °C) being reached after 4 min in the absence of any catalyst (Fig. 8B and C). The ¹H-NMR analysis of the model reaction confirmed 70% epoxide conversion after 15 min of reaction with the formation of the corresponding adduct (Fig. S26†). However, under the foaming conditions, bismuthiol (T2) was not able to directly react with the epoxide because the thiol/amine acid–base reaction took place very rapidly, leading to the corresponding salt, which was unable to react with the epoxide. This was proved by first reacting bismuthiol (T2) with an excess of amine (SH/NH₂ = 1/3, a similar composition to that in the foam formulation) before adding the epoxide. In these conditions, no exotherm (green curve in Fig. 8B for T2) was observed and almost no conversion of the epoxide by the thiol was observed by ¹H-NMR spectroscopy (Fig. 8C, T2 amine-salt) at r.t. Whereas thiols are able to oxidize and form disulfide bonds under basic conditions, model reaction studies carried out in the presence of amines did not show the occurrence of this reaction under the foaming conditions (see section 2.4 for a detailed discussion, and Fig. S28 and S29† for ¹H-NMR studies).

Despite the difficulty of fully determining the relative kinetics of all possible reactions, we hypothesized that the thiol-amine acid–base reaction was the first to take place, thus promoting the first exotherm needed to initiate the aminolysis of the epoxide. The stable thiol-amine salt limited the reaction of the thiol with the epoxide and 5CC, until the temperature reached 80–100 °C at which salt dissociation was expected to occur. Beyond 100 °C, the thiol reacted with 5CC to generate CO₂ and with the epoxide.

We then investigated the versatility of the process. Through careful selection of the amine and epoxide components in the formulation, it was possible to achieve both flexible and rigid foams. As expected, the most rigid foam was obtained by combining the most rigid amine (XDA) with the aromatic epoxide monomer (DER 332), resulting in a foam with a *T_g* of 49 °C (F11, Fig. 6B). The compressive curve of this foam exhibited plastic deformation behaviour,^{47,48} with a modulus of 81 MPa, a yield stress of approximately 3 MPa, and an almost zero plateau beyond the yield stress (green curve, Fig. 6C). Substituting the aromatic epoxide in this formulation with an aliphatic one (BDGE) significantly altered the characteristics of the foam. The resulting foam (F8) exhibited a *T_g* value of 28 °C and a compressive modulus of 5 MPa, consistent with the properties of a semi-rigid foam (Fig. 6). Additionally, replacing XDA with the cyclo-aliphatic amine produced a foam (F9) with a similar *T_g* value but with an enhanced compressive modulus (23.5 MPa) for a similar density (Fig. 6). The properties of foam F7 obtained from the other aromatic thiol T3 are in line with these values (a *T_g* value of 28 °C and a compressive

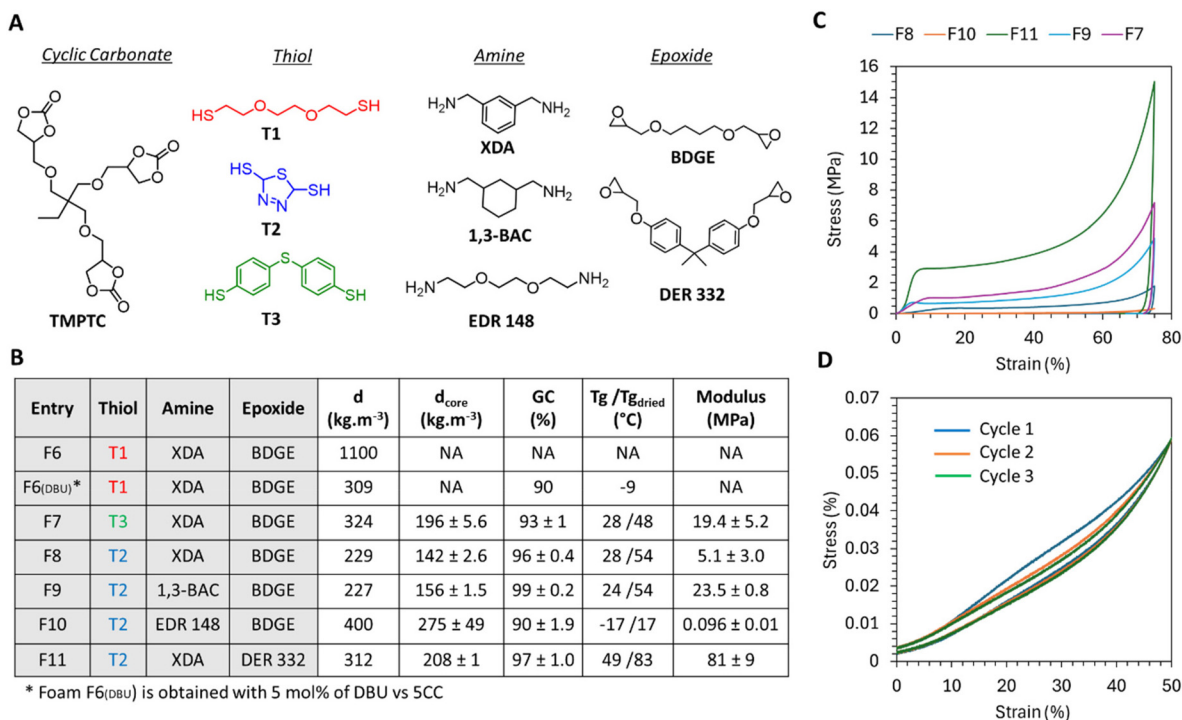


Fig. 6 Foaming from r.t. formulations under catalyst free conditions and foam properties. (A) Structure of the component involved in the different formulations. (B) Composition of the formulations and properties of the foams. (C) Compressive curve of the foams synthesized with T2. (D) Three consecutive loading–unloading cycles of F10 at an initial compressive rate = 0.0025 s⁻¹. DSC thermograms are presented in Fig. S17–S22 in the ESI.† Conditions: TMPTC, epoxide, amine, thiol, [5CC] : [epoxide] : [NH_{2 total}] : [SH] = 1 : 1 : 1.5 : 0.5. d states for the density measured on the whole foam, and d_{core} states for the density measured at the center of the foam.

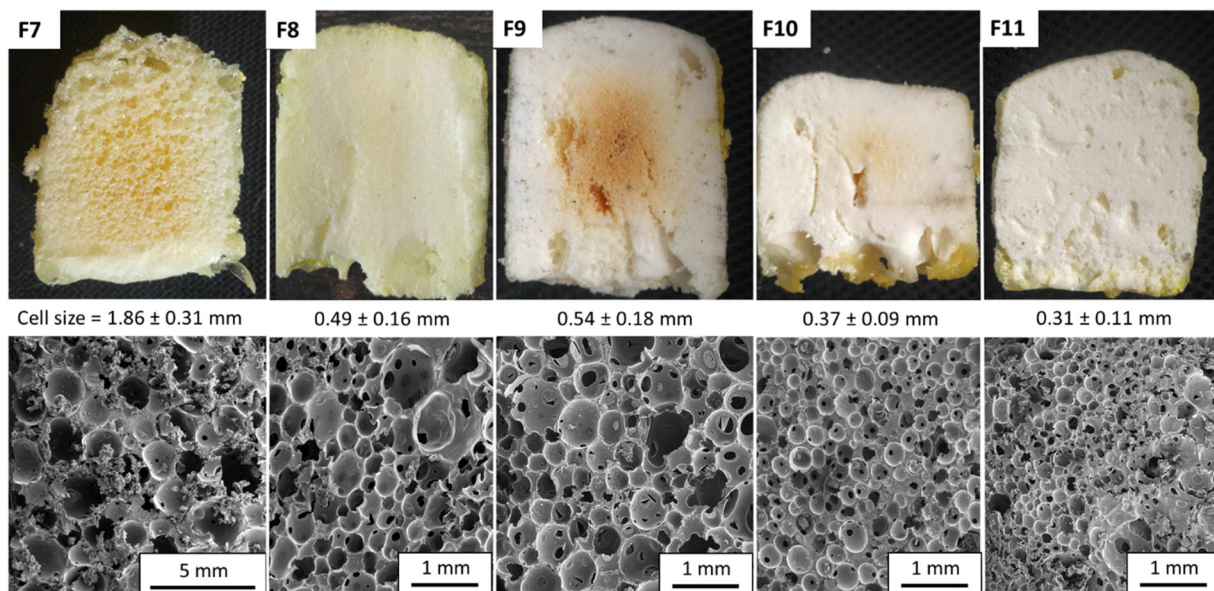


Fig. 7 Images and SEM of the different foams obtained from r.t. formulations under catalyst free conditions. Conditions: TMPTC, epoxide, amine, thiol with [5CC] : [epoxide] : [NH_{2 total}] : [SH] = 1 : 1 : 1.5 : 0.5, foaming RT.

modulus of 19.4 MPa; Fig. 6). We observed that aromatic thiols played a crucial role in achieving rigid or semi-rigid foams. For the sake of comparison, the foam F6_{DBU} produced from the ali-

phatic thiol (T1), XDA, and BDGE in the presence of DBU exhibited a low T_g value of -9 °C together with a low modulus of 0.0192 MPa, resulting in a foam that was significantly more

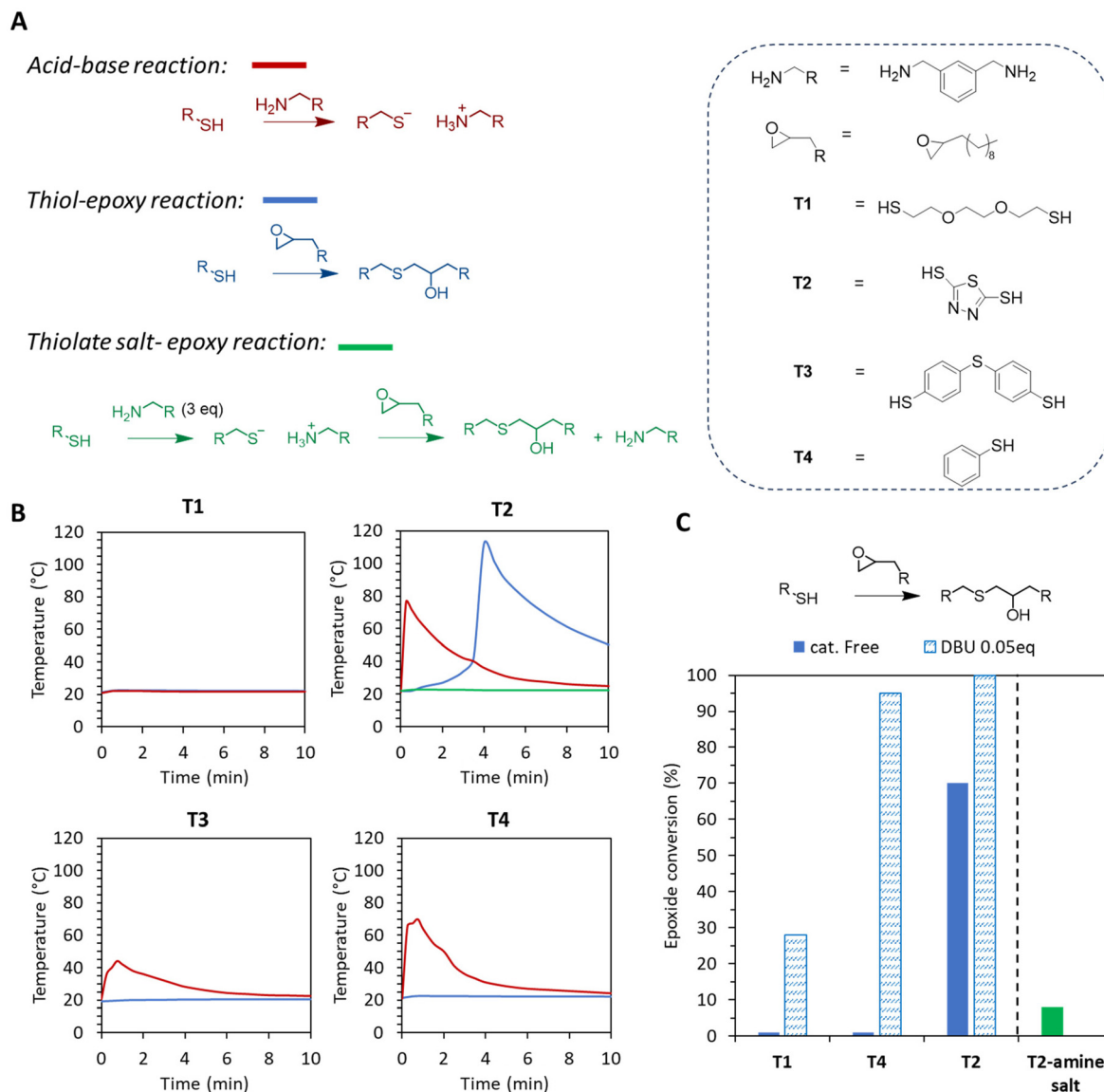


Fig. 8 Model reaction of a thiol with an epoxide and/or amine. (A) Scheme of the three considered reactions. (B) Exotherm for the three reactions. (C) Epoxide conversion after the reaction of the model epoxide with different thiols and the thiol amine salt. Conditions: acid-base reaction [epoxide]/[NH₂] = 1 : 1, thiol-epoxy reaction : [epoxide]/[SH] = 1 : 1, and thiolate salt-epoxy reaction [epoxide]/[SH]/[NH₂] = 1 : 1 : 3. ¹H-NMR spectra are presented in Fig. S23–S27 in the ESI.†

flexible than the ones discussed in this section (Fig. S30†). Note that in all cases, foams were hydroplasticized by moisture, a common feature for PHU.^{13,28,29,31,49,50}

We also investigated the influence of the epoxide structure on foaming. For this purpose, we substituted BDGE with epoxidized soybean oil (ESBO) featuring internal epoxides instead of external ones. Despite being of great interest due to the good availability and biobased origin of such internal epoxides, the low reactivity of the internal epoxides did not allow generation of a large exotherm and thus, induction of foaming. Indeed, only a temperature of 42.9 °C was reached when using ESBO instead of BDGE (Fig. S31C†) under similar foaming conditions. The reaction of the thiol with the internal

epoxides was also tested using a model reaction between bis-muthiol and ESBO. Bismuthiol reacted slowly with ESBO with the formation of 17% thioether linkage (Fig. S31A†) after 15 min without any catalyst at room temperature with a very slight exotherm (Fig. S31B†) compared to 70% thioether bonding when reacting with 1,2-epoxydodecane (Fig. 8C).

Finally, the combination of both an aliphatic amine (EDR 148) and an aliphatic epoxide (BDGE) resulted in the flexible foam **F10**, as evidenced by a *T_g* value below room temperature (−17 °C) and a low modulus of 0.096 MPa (Fig. 6). The compressive curve in Fig. 6C shows a constant plateau modulus beyond the elastic region and the foam was able to recover its shape after compression with a small amount of hysteresis

loss (hysteresis loss = 17% for 50% compression strain; Fig. 6D). By repeating the compression cycle 2 more times, we observed that the modulus during loading decreased from 0.1071 to 0.088 MPa between the first and second cycle and there was an almost full recovery of the modulus between cycles 2 and 3 (0.0844 MPa). In contrast, the unloading curves superimposed quite well and then showed hysteresis losses of 12.8 and 11.5% during unloading respectively for cycles 2 and 3.

4. Conclusions

Thiol-induced self-blown non-isocyanate polyurethane (NIPU) foams are promising CO₂-sourced alternatives to conventional isocyanate-based foams. However, their production is still slow (*i.e.* 30 min at 120 °C), far from the 1–10 minutes required for many industrial foaming processes. Herein, we investigated the reasons for these slow processes, and developed optimized strategies for the production of NIPU foams in short time frames (5 minutes) notably by replacing aliphatic thiols with aromatic ones. Remarkably, as aromatic thiols are more acidic than aliphatic ones, the amine comonomer was basic enough to catalyze the *S*-alkylation, thus leading to fast foaming (5 min) at 100 °C without requiring an organobase catalyst (DBU) as is commonly used in the original process. Since the system was not sufficiently reactive for room temperature foaming, the cascade exotherm strategy employed for the water-induced self-foaming process was then implemented to rapidly raise the formulation temperature to the foaming zone in minutes. Model reactions showed that the higher acidity of the aromatic thiol led to a strong acid–base reaction with the amine comonomer. This first exothermic reaction allowed initiation of the other ones (*i.e.* the aminolysis of the cyclic carbonates and epoxides). This cascade exotherm enabled the foaming zone to be reached very quickly, delivering stable crosslinked NIPU foams in 5 minutes under catalyst-free conditions from *r.t.* formulations. With aliphatic thiols, a strong organobase catalyst (DBU) was needed to achieve such a foaming performance. More than accelerating the foaming, aromatic thiols allowed much more freedom to prepare foams of very distinct properties. Indeed, by the choice of the amine comonomer and epoxide, flexible, semi-rigid or rigid foams presenting *T_g* values from –17 to 49 °C were easily accessible, such versatility not being possible with the aliphatic thiol.

This work shows that, by a careful understanding of the foaming process, simple strategies can be implemented to tackle the low reactivity of cyclic carbonates for the fast self-blowing of solvent-free NIPU formulations, offering potential retrofitting of existing PU foam production plants.

Author contributions

Maxime Bourguignon carried out the experimental design, data analysis and manuscript writing. Bruno Grignard synthesized the cyclic carbonate, and participated in result discus-

sions and manuscript correction. Christophe Detrembleur obtained the funding resources, supervised the project, and participated in result discussions and manuscript correction.

Data availability

Supplementary data for this article, including DSC thermograms, infrared spectra, ¹H NMR spectra, supplementary syntheses, and cyclic carbonate synthesis, are present in the ESI.†

Conflicts of interest

There are no conflicts to declare.

Acknowledgements

The authors thank the Region Wallonne for funding the Win2Wal project “ECOFOAM” (convention 2010130). They also thank the company NMC sa (Belgium) for their support in this research. The authors are very grateful to Grégory Cartigny for technical assistance in the preparation of the formulations and the foams. Christophe Detrembleur is the FNRS Research Director and thanks the Fonds de la Recherche Scientifique (F. R.S.-FNRS) for funding. Christophe Detrembleur is particularly grateful to the Region Wallonne for funding the FRFS-WEL-T project Chemistry (convention WEL-T-CR-2023 A).

References

- 1 J. O. Akindoyo, M. D. H. Beg, S. Ghazali, M. R. Islam, N. Jeyaratnam and A. R. Yuvaraj, *RSC Adv.*, 2016, **6**, 114453–114482.
- 2 H.-W. Engels, H.-G. Pirkel, R. Albers, R. W. Albach, J. Krause, A. Hoffmann, H. Casselmann and J. Dormish, *Angew. Chem., Int. Ed.*, 2013, **52**, 9422–9441.
- 3 <https://www.imargroup.com/polyurethane-foam-market>.
- 4 J. Peyrton and L. Avérous, *Mater. Sci. Eng., R*, 2021, **145**, 100608.
- 5 M. H. Karol and J. A. Kramarik, *Toxicol. Lett.*, 1996, **89**, 139–146.
- 6 D. Bello, C. A. Herrick, T. J. Smith, S. R. Woskie, R. P. Streicher, M. R. Cullen, Y. Liu and C. A. Redlich, *Environ. Health Perspect.*, 2007, **115**, 328–335.
- 7 S. Merenyi, *REACH: Regulation (EC) No 1907/2006: Consolidated version (June 2012) with an introduction and future prospects regarding the area of Chemicals legislation (Vol. 2)*, GRIN Verlag.
- 8 European Commission, *Communication from the commission to the European Parliament and the council, Sustainable carbon cycles*, Brussels, 2021.
- 9 C. Carré, Y. Ecochard, S. Caillol and L. Avérous, *ChemSusChem*, 2019, **12**, 3410–3430.

- 10 B. Grignard, S. Gennen, C. Jérôme, A. W. Kleij and C. Detrembleur, *Chem. Soc. Rev.*, 2019, **48**, 4466–4514.
- 11 F. D. Bobbink, A. P. van Muyden and P. J. Dyson, *Chem. Commun.*, 2019, **55**, 1360–1373.
- 12 T. Theerathanagorn, T. Kessaratikoon, H. U. Rehman, V. D'Elia and D. Crespy, *Chin. J. Chem.*, 2024, **42**, 652–685.
- 13 P. Sen Choong, N. X. Chong, E. K. Wai Tam, A. M. Seayad, J. Seayad and S. Jana, *ACS Macro Lett.*, 2021, **10**, 635–641.
- 14 G. Seychal, P. Nickmilder, V. Lemaury, C. Ocando, B. Grignard, P. Leclère, C. Detrembleur, R. Lazzaroni, H. Sardon, N. Aranburu and J.-M. Raquez, *Composites, Part A*, 2024, **185**, 108311.
- 15 G. Seychal, C. Ocando, L. Bonnaud, J. De Winter, B. Grignard, C. Detrembleur, H. Sardon, N. Aranburu and J.-M. Raquez, *ACS Appl. Polym. Mater.*, 2023, **5**, 5567–5581.
- 16 P. Helbling, F. Hermant, M. Petit, T. Tassaing, T. Vidil and H. Cramail, *Polym. Chem.*, 2023, **14**, 500–513.
- 17 A. Gomez-Lopez, F. Elizalde, I. Calvo and H. Sardon, *Chem. Commun.*, 2021, **57**, 12254–12265.
- 18 A. Gomez-Lopez, S. Panchireddy, B. Grignard, I. Calvo, C. Jerome, C. Detrembleur and H. Sardon, *ACS Sustainable Chem. Eng.*, 2021, **9**, 9541–9562.
- 19 F. Magliozzi, A. Scali, G. Chollet, D. Montarnal, E. Grau and H. Cramail, *ACS Sustainable Chem. Eng.*, 2020, **8**, 9125–9135.
- 20 H. Blattmann, M. Lauth and R. Mülhaupt, *Macromol. Mater. Eng.*, 2016, **301**, 944–952.
- 21 B. Grignard, J.-M. Thomassin, S. Gennen, L. Poussard, L. Bonnaud, J.-M. Raquez, P. Dubois, M.-P. Tran, C. B. Park, C. Jerome and C. Detrembleur, *Green Chem.*, 2016, **18**, 2206–2215.
- 22 T. Dong, E. Dheressa, M. Wiatrowski, A. P. Pereira, A. Zeller, L. M. L. Laurens and P. T. Pienkos, *ACS Sustainable Chem. Eng.*, 2021, **9**, 12858–12869.
- 23 C. Amezúa-Arranz, M. Santiago-Calvo and M.-Á. Rodríguez-Pérez, *Eur. Polym. J.*, 2023, **197**, 112366.
- 24 A. Cornille, S. Dworakowska, D. Bogdal, B. Boutevin and S. Caillol, *Eur. Polym. J.*, 2015, **66**, 129–138.
- 25 A. Cornille, C. Guillet, S. Benyahya, C. Negrell, B. Boutevin and S. Caillol, *Eur. Polym. J.*, 2016, **84**, 873–888.
- 26 G. Coste, M. Denis, R. Sonnier, S. Caillol and C. Negrell, *Polym. Degrad. Stab.*, 2022, **202**, 110031.
- 27 G. Coste, C. Negrell, L. Averous and S. Caillol, *ACS Sustainable Chem. Eng.*, 2022, **10**, 8549–8558.
- 28 M. Bourguignon, B. Grignard and C. Detrembleur, *Angew. Chem., Int. Ed.*, 2022, **61**, e202213422.
- 29 D. Trojanowska, F. Monie, G. Perotto, A. Athanassiou, B. Grignard, E. Grau, T. Vidil, H. Cramail and C. Detrembleur, *Green Chem.*, 2024, **26**, 8383–8394.
- 30 M. Bourguignon, B. Grignard and C. Detrembleur, *J. Am. Chem. Soc.*, 2024, **146**, 988–1000.
- 31 F. Monie, B. Grignard and C. Detrembleur, *ACS Macro Lett.*, 2022, **11**, 236–242.
- 32 F. Monie, B. Grignard, J.-M. Thomassin, R. Mereau, T. Tassaing, C. Jerome and C. Detrembleur, *Angew. Chem., Int. Ed.*, 2020, **59**, 17033–17041.
- 33 G. Coste, C. Negrell and S. Caillol, *Macromol. Rapid Commun.*, 2022, **43**, 2100833.
- 34 N. S. Purwanto, Y. Chen and J. M. Torkelson, *ACS Appl. Polym. Mater.*, 2023, **5**, 6651–6661.
- 35 N. S. Purwanto, Y. Chen, T. Wang and J. M. Torkelson, *Polymer*, 2023, **272**, 125858.
- 36 M. Chaib, S. El Khezraji, S. Thakur, H. Ben Youcef, M. Lahcini and R. Verdejo, *React. Funct. Polym.*, 2024, **200**, 105924.
- 37 B. Li and R. M. Aspden, *J. Bone Miner. Res.*, 1997, **12**, 641–651.
- 38 S. Wang, W. Liu, D. Yang and X. Qiu, *Ind. Eng. Chem. Res.*, 2019, **58**, 496–504.
- 39 B. Grignard, P. Mampuy, J. Escudero, D. Masullo, F. Lemièrre, B. U. W. Maes and C. Detrembleur, *Polym. Chem.*, 2022, **13**, 6599–6605.
- 40 N. S. Purwanto, Y. Chen and J. M. Torkelson, *Eur. Polym. J.*, 2024, **206**, 112775.
- 41 Y. Hu, C.-Y. Li, X.-M. Wang, Y.-H. Yang and H.-L. Zhu, *Chem. Rev.*, 2014, **114**, 5572–5610.
- 42 Z. Yao, B. Dai, Y. Yu, H. Ji, L. Zhou and K. Cao, *RSC Adv.*, 2017, **7**, 10881–10884.
- 43 K. Jin, W. H. Heath and J. M. Torkelson, *Polymer*, 2015, **81**, 70–78.
- 44 A. O. Konuray, X. Fernández-Francos and X. Ramis, *Polymer*, 2017, **116**, 191–203.
- 45 T. H. Lee, Y. Il Park, S. M. Noh and J. C. Kim, *Prog. Org. Coat.*, 2017, **104**, 20–27.
- 46 T. Habets, F. Siragusa, A. J. Müller, Q. Grossman, D. Ruffoni, B. Grignard and C. Detrembleur, *Polym. Chem.*, 2022, **13**, 3076–3090.
- 47 Z. H. Tu, V. P. W. Shim and C. T. Lim, *Int. J. Solids Struct.*, 2001, **38**, 9267–9279.
- 48 F. Rahimidehgolan and W. Altenhof, *Composites, Part B*, 2023, **253**, 110513.
- 49 C. Pronoitis, M. Hakkarainen and K. Odelius, *ACS Sustainable Chem. Eng.*, 2022, **10**, 2522–2531.
- 50 I. Łukaszewska, A. Bukowczan, K. N. Raftopoulos and K. Pieliowski, *Polymer*, 2024, **302**, 127060.